

MD study on high-energy reactive cluster impact on diamond (111) and (100) surfaces

Y. Yamaguchi^{1,a} and J. Gspann²

¹ Department of Mechanical Engineering, Osaka University, 2-1 Yamadaoka, Suita 565-0871, Japan

² Institut für Mikrostrukturtechnik, Universität and Forschungszentrum Karlsruhe, Postfach 3640, 76021 Karlsruhe, Germany

Received 6 September 2004

Published online 13 July 2005 – © EDP Sciences, Società Italiana di Fisica, Springer-Verlag 2005

Abstract. Molecular dynamics (MD) simulations of single argon, CO₂ and O₂ cluster impacts on diamond (100) and (111) surfaces are performed in order to investigate the surface erosion process. The transient crater on the (100) surface seems rather unphpherical and skew compared to the typical hemispherical crater appeared on the (111) surface due to the orientation-dependent hardness. Argon cluster impacts on the diamond (100) surface resulted in a slightly higher erosion rate than on the (111) surface while it is lowered on the (111) surface for CO₂ cluster impacts. The difference in the susceptibility to the physical erosion appears in the rim or the crater.

PACS. 79.20.Rf Atomic, molecular, and ion beam impact and interactions with surfaces – 31.15.Qg Molecular dynamics and other numerical methods

1 Introduction

Highly accelerated ionized cluster beams may be applied as a physical as well as chemical erodant for micro- and nano-scale surface structuring [1–4], where clusters consisting of about 1000 CO₂ molecules are accelerated to up to 100 keV/cluster and continuously impact on surfaces of diamond, silicon, glass, and Teflon films. The reactive enhancement of the surface erosion was clearly shown in the difference in the erosion rates between CO₂ and argon cluster impacts, with a factor of 3.63 in the case of synthetic diamond, while the eroded surface was remarkably smoother for the argon cluster impact [3]. The differences in the erosion effect or roughness of eroded surfaces between natural diamond and synthetic diamond (Monodite) were also indicated.

The authors have also performed molecular dynamics (MD) simulations of single Ar_{*n*}, (CO₂)_{*n*}, fictious (C₃)_{*n*}, and (O₂)_{*m*} (*n* ≈ 960, *m* = 960, 1440) cluster impacts on a diamond (111) surface [5–8]. For single argon and CO₂ cluster impacts with an acceleration energy E_a of 100 keV/cluster, the formation of a hemispherical crater and induced shockwaves were observed at the early stage of the impact process. Rebounding hot fluidized carbon material was then seen to replenish the transient crater very quickly until 2 ps, with a central peak appearing as a long time phenomenon only for a CO₂ cluster impact. The reactive enhancement of the surface erosion via the CO₂ cluster impact was only achieved for $E_a \geq 75$ keV where the difference in the erosion effect between argon

and CO₂ cluster impacts became remarkable, whereas the surface of the relaxed crater was more densely packed and smoother for the argon cluster impact [6]. Unlike these impacts, the (O₂)₁₄₄₀ cluster impact induced a significant effect from a lower impact energy E_a of 30 keV on, and the erosion rate increased almost linearly with the increase of the impact energy [8]. These differences were ascribed to the reactive emission pattern via the production of CO and CO₂ molecules. In addition, the comparison between (O₂)₁₄₄₀ and (O₂)₉₆₀ impacts indicated that the erosion rate per molecule seemed to be expressed as a linear function of the impact velocity minus a threshold velocity independent of the cluster size for the (O₂) cluster impacts.

In this report, MD simulations of argon, CO₂, and O₂ cluster impacts on a diamond (100) surface are performed with the acceleration energy E_a up to 100 keV/cluster, and compared with impacts on a diamond (111) surface regarding the erosion rate and surface structure.

2 Simulation method

The simulation methods applied are almost the same as in our previous reports [5–8]. Briefly the empirical potential function proposed by Brenner [9] is adopted for the interaction among carbon atoms with a slight simplification, while the interaction potentials of C–O and O–O are derived appropriately from Brenner’s formula [6]. Lennard-Jones potentials are adopted for C–Ar and Ar–Ar interactions. A cylindrical single crystal is applied as the impact target of a diamond (100) surface

^a e-mail: yamaguchi@mech.eng.osaka-u.ac.jp

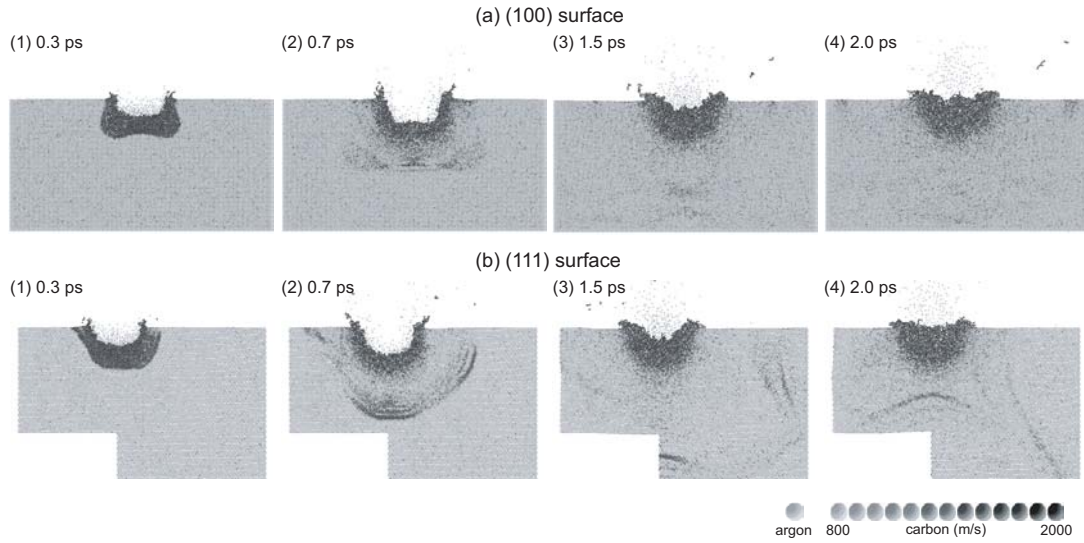


Fig. 1. Comparison of the snapshots of the Ar_{961} cluster impacts on the (100) (upper) and (111) (lower) diamond surfaces with the acceleration energy E_a of 100 keV (/cluster) until 2 ps after the impact. A cross-section parallel to the impact direction with a thickness of 10 Å is shown, and carbon atoms with larger velocity have darker shade.

which consists of 1,997,307 carbon atoms. Both the depth parallel to the impact direction and the radius of the cylinder are about 153 Å, and the system size is about 17% smaller in the length scale than that for the simulation on the (111) surface in which the number of carbon atoms was reduced by applying a technique considering the crystal symmetry [5–8]. However, the smaller region size is not crucial in the sense that unlike in the case of the (111) surface, there is no reflected shockwave directly returning back to the impact point for the (100) surface because there is no shockwave propagation direction parallel to the impact direction of (100) [6,7]. The temperature is kept fixed at 300 K near the outer boundary with the Langevin method. The impacting argon and CO_2 clusters contain about 1000 molecules (Ar_{961} , $(\text{CO}_2)_{960}$), in accordance with the experiment [1–3], while $(\text{O}_2)_{1440}$ cluster is adopted for the comparison so that the total number of atoms in the impacting cluster is the same. The size effect for the O_2 cluster impact has already been examined in a previous report [8].

3 Results and discussions

Figure 1 shows the comparison of the snapshots of the Ar_{961} cluster impacts on the (100) and (111) diamond surfaces with the acceleration energy E_a of 100 keV (/cluster) until 2 ps after the impact. A cross-section parallel to the impact direction with a thickness of 10 Å is shown, and carbon atoms with larger velocity have darker shade. The cluster crushes into the diamond surface [Fig. 1 (a1, b1)] and a transient crater structure develops until about 0.7 ps after the impact [Fig. 1 (a2, b2)]. The crater on the (100) surface seems rather unspherical and skew compared to the typical hemispherical crater appearing on the (111) surface presumably due to the orientation-dependent hardness which also induces the unspherical

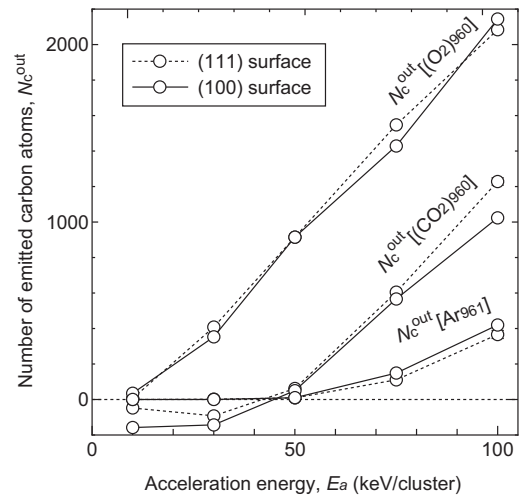


Fig. 2. Comparison of diamond (100) and (111) surfaces in the net number of emitted carbon atoms N_C^{out} calculated as the offset from the initial value for single Ar_{961} , $(\text{CO}_2)_{960}$ and $(\text{O}_2)_{1440}$ cluster impacts at $10 \leq E_a \leq 100$ keV.

shockwave propagation described below. The crater is however immediately filled up with the fluidized hot carbon material compressed around the impact crater due to the elastic recovery in both cases [Fig. 1 (a3, b3)] and there remains no apparent crater already about 2.0 ps after the impact [Fig. 1 (a4, b4)]. As mentioned in Section 2, the impact induced shockwaves propagate in specific directions, i.e., $(\bar{1}\bar{1}\bar{1})$, $(\bar{1}\bar{1}\bar{1})$, $(\bar{1}\bar{1}\bar{1})$ and $(\bar{1}\bar{1}\bar{1})$ directions for the (111) surface, and $(\bar{1}\bar{1}\bar{1})$, $(\bar{1}\bar{1}\bar{1})$, $(\bar{1}\bar{1}\bar{1})$ and $(\bar{1}\bar{1}\bar{1})$ directions for the (100) surface, thus no reflected shockwave directly returning back to the impact point can be seen in the case of the (100) surface.

Figure 2 denotes the comparison of diamond (100) and (111) surfaces in the net number of emitted carbon

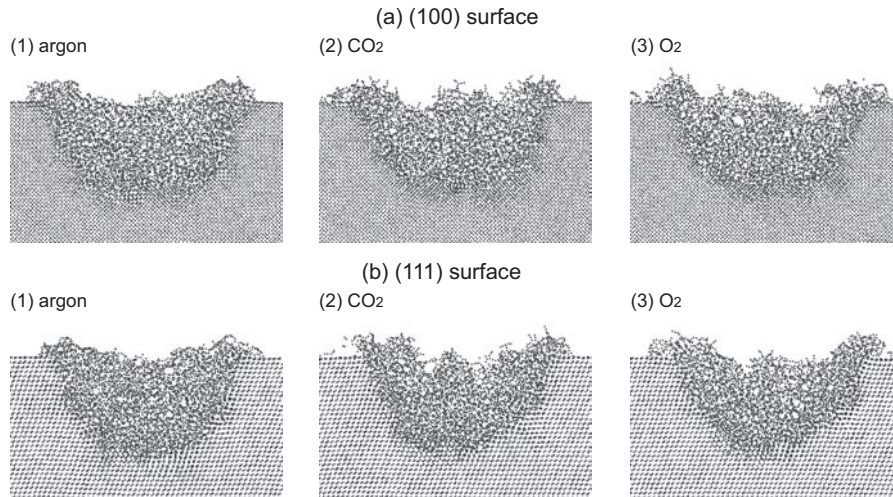


Fig. 3. Comparison of the enlarged snapshots of the relaxed crater at 30 ps after single impacts of Ar_{961} , $(\text{CO}_2)_{960}$, and $(\text{O}_2)_{1440}$ clusters on diamond (100) and (111) surfaces at $E_a = 100$ keV.

atoms N_c^{out} calculated as the offset from the initial value (see Ref. [6]) for single Ar_{961} , $(\text{CO}_2)_{960}$ and $(\text{O}_2)_{1440}$ cluster impacts at $10 \leq E_a \leq 100$ keV. Concerning the Ar_{961} impact, the erosion rate is higher for the (100) surface for $E_a \geq 75$ keV, and this difference is ascribed to the surface property that the (100) surface is more susceptible to the physical erosion than the (111) surface. This susceptibility is also related to the difference in the surface roughness [3] or the friction [4] observed in the experiment, or the rather skew structure of the transient crater shown in Figure 1 (a1, a2). On the contrary, the erosion rate for the $(\text{CO}_2)_{960}$ is always lower on the (100) surface. Considering that the erosion effect for the $(\text{O}_2)_{1440}$ on both surfaces are almost the same, the carbon atoms in the impacting CO_2 cluster may easier be deposited on the (100) surface, and that results in the lower net erosion effect.

Figure 3 exhibits the comparison of the enlarged snapshots of the relaxed crater at 30 ps after the single impact of Ar_{961} , $(\text{CO}_2)_{960}$, and $(\text{O}_2)_{1440}$ clusters on diamond (100) and (111) surfaces at $E_a = 100$ keV. The relaxed crater was densely packed and smoother for the argon cluster impact on both (100) and (111) surfaces [Fig. 3 (a1, b1)], while the rim of the crater seems slightly larger on the (100) surface indicating the higher susceptibility to the physical erosion. Interestingly, the roughness or hillock seems more remarkable for CO_2 cluster impacts than for O_2 especially near the center of the impact point. Considering that the central peak is the residue of the fluidized hot carbon material formed in the intense upward flow during the crater recovery, ample oxygen supply via the O_2 cluster impact may easily terminate the dangling bonds and decompose the fluidized carbon material into inactive CO or CO_2 leading to a less residue.

4 Conclusions

MD simulations of single argon, CO_2 and O_2 cluster impacts on diamond (111) and (100) surfaces are performed in order to investigate the surface erosion process. The transient crater on the (100) surface seems rather unspherical and skew compared to the typical hemispherical crater appearing on the (111) surface due to the orientation-dependent hardness. The argon cluster impacts on the diamond (100) surface resulted in a slightly higher erosion rate than on the (111) surface while it is lowered on the (111) surface for the CO_2 cluster. The difference in the susceptibility to the physical erosion is evident in the rim or the crater.

References

1. A. Gruber, J. Gspann, H. Hoffmann, Appl. Phys. A **68**, 197 (1999)
2. C. Becker, J. Gspann, R. Krämer, Eur. Phys. J. D **16**, 301 (2001)
3. R. Krämer, Y. Yamaguchi, J. Gspann, Surf. Interface Anal. **36**, 148 (2004)
4. R. Krämer, Y. Yamaguchi, J. Gspann, Eur. Phys. J. D **34**, 235 (2005)
5. Y. Yamaguchi, J. Gspann, Eur. Phys. J. D **16**, 105 (2001)
6. Y. Yamaguchi, J. Gspann, Phys. Rev. B **66**, 155408 (2002)
7. Y. Yamaguchi, J. Gspann, Eur. Phys. J. D **24**, 315 (2003)
8. Y. Yamaguchi, J. Gspann, Nucl. Instr. Meth. Phys. Res. B **228**, 309 (2005)
9. D.W. Brenner, Phys. Rev. B **42**, 9458 (1992)